9460 *Inorg. Chem.* **2010**, *49*, 9460–9469
DOI: 10.1021/ic1011428

Inorganic Chemistry
Article

cis-Dioxo- and *cis*-(Hydroxo)oxo-Mo(V) Complexes Stabilized by Intramolecular Hydrogen-Bonding

Victor W. L. Ng,[†] Michelle K. Taylor,[†,‡] Jonathan M. White,[†,‡] and Charles G. Young*,[†]

[†]*School of Chemistry and* [‡]*Bio21 Molecular Science and Biotechnology Institute, University of Melbourne, Victoria 3010, Australia*

Received June 7, 2010

The reactions of $Tp^{iPr}Mo^{VI}O_2Cl$ with salicylanilides and NEt_3 produce *cis*-$Tp^{iPr}Mo^{VI}O_2(2\text{-}OC_6H_4CONHR)$ (Tp^{iPr} = hydrotris(3-isopropylpyrazol-1-yl)borate, R = Ph, 4-C_6H_4Cl, 4-C_6H_4OMe). The *N*-methyl complex, $Tp^{iPr}MoO_2\{2\text{-}OC_6H_4CON(Me)Ph\}$, is similarly prepared. Reduction of the amido complexes by cobaltocene produces green, EPR-active compounds, $[CoCp_2][Tp^{iPr}Mo^{V}O_2(2\text{-}OC_6H_4CONHR)]$, that exhibit strong, low energy, $\nu(MoO_2)$ IR bands at $\sim$ 895 and 790 cm^{-1} (cf. $\sim$ 935 and 900 cm^{-1} for the Mo(VI) analogues). The X-ray structures of all seven complexes have been determined. In each case, the Mo center exhibits a distorted octahedral coordination geometry defined by mutually *cis* oxo and phenolate ligands and a tridentate *fac*-Tp^{iPr} ligand. The Mo(V) anions exhibit greater Mo═O distances (av. 1.738 Å vs 1.695 Å) and O═Mo═O angles (av. 112.4° vs 102.9°) than their Mo(VI) counterparts, indicative of the presence of a three-center (MoO_2), π^* semioccupied molecular orbital in these d^1 complexes. The amido Mo(VI) and Mo(V) complexes exhibit an intramolecular hydrogen-bond between the N*H* and $O_{phenolate}$ atoms. Protonation of $[CoCp_2][Tp^{iPr}Mo^{V}O_2(2\text{-}OC_6H_4CONHR)]$ by lutidinium tetrafluoroborate is quantitative and produces EPR-active, *cis*-(hydroxo)oxo-Mo(V) complexes, $Tp^{iPr}Mo^{V}O(OH)(2\text{-}OC_6H_4CONHR)$, related to the low pH Mo(V) forms of sulfite oxidase.

Introduction

Oxo complexes and their chemical reactions dominate the high-valent chemistry of the early and middle transition metals and underpin applications and progress in diverse fields,[1−3] especially materials science and technology[4−7] and chemical[8−12] and biological[12−14] catalysis. Consistent with the strong π-base character of the oxo ligand[1] and Pauling's electroneutrality principle,[15] only high oxidation state metal ions form stable oxo complexes. Apart from some notable exceptions, particularly in Ru and Os chemistry,[16,17] only metal ions in their highest oxidation state can support two or more oxo ligands.

Complexes with unusual oxo ligand number/oxidation state combinations display unique physical and chemical properties and many have found applications in chemical, electrochemical and photochemical oxidation processes. This is most evident in the ability of Cr(V),[18] Mn(V),[18] Fe(IV),[19,20]

*To whom correspondence should be addressed. E-mail: cgyoung@unimelb.edu.au.

(1) Nugent, W. A.; Mayer, J. M. *Metal-Ligand Multiple Bonds*; Wiley: New York, 1988.
(2) *Comprehensive Coordination Chemistry*; Wilkinson, G., McCleverty, J. A., Gillard, R. D., Eds.; Pergamon: Oxford, U.K., 1987, Vols. *3, 4*.
(3) *Comprehensive Coordination Chemistry II*; McCleverty, J. A., Meyer, T. J., Eds.; Elsevier Pergamon: Amsterdam, 2004; Vols. *4, 5, 8*.
(4) Jolivet, J.-P. *Metal Oxide Chemistry and Synthesis: From Solution to Solid State*; Wiley: Chichester, U.K., 2000.
(5) Mann, S. *Biomineralization: Principles and Concepts in Biological Materials Chemistry*; Oxford University: Oxford, U.K., 2001.
(6) (a) *Polyoxometalate Chemistry for Nano-Composite Design*; Yamase, T., Pope, M. T., Eds.; Kluwer: New York, 2002. (b) *Polyoxometalate Molecular Science*; Borrás-Almenar, J. J., Coronado, E., Müller, A., Pope, M., Eds.; NATO Science Series II, Vol. *98*; Kluwer: Dordrecht, The Netherlands, 2003.
(7) Ozin, G. A.; Arsenault, A. C.; Cademartiri, L. *Nanochemistry: a Chemical Approach to Nanomaterials*, 2nd ed.; Royal Society of Chemistry: Cambridge, U.K., 2009.
(8) Holm, R. H. *Chem. Rev.* **1987**, *87*, 1401–1449.
(9) (a) Sheldon, R. A.; Kochi, J. K. *Metal−Catalysed Oxidation of Organic Compounds*; Academic: New York, 1981. (b) *Catalytic Oxidation: Principles and Applications*; Sheldon, R. A., van Santen, R. A., Eds.; World Scientific: Singapore, 1995.
(10) *Modern Oxidation Methods*; Bäckvall, J.-E., Ed.; Wiley-VCH: Weinheim, 2004.
(11) Gunay, A.; Theopold, K. H. *Chem. Rev.* **2010**, *110*, 1060–1081.
(12) *Biomimetic Oxidations Catalyzed by Transition Metal Complexes*; Meunier, B., Ed.; Imperial College Press: London, U.K., 2000.
(13) Holm, R. H. *Coord. Chem. Rev.* **1990**, *100*, 183–221.
(14) Bertini, I.; Gray, H. B.; Stiefel, E. I.; Valentine, J. S. *Biological Inorganic Chemistry: Structure and Reactivity*; University Science Books: Sausalito, CA, 2007.
(15) Pauling, L. *The Nature of the Chemical Bond*, 3rd ed.; Cornell University: Ithaca, NY, 1960; pp 172−174.
(16) Che, C.-M.; Yam, V. W.-W. *Adv. Inorg. Chem.* **1992**, *39*, 233–325.
(17) Che, C.-M.; Lau, T.-C. In *Comprehensive Coordination Chemistry II*; McCleverty, J. A., Meyer, T. J., Eds.; Elsevier Pergamon: Amsterdam, 2004, Vol. *5*; Chap 5.6, pp 733−847.
(18) McGarrigle, E. M.; Gilheaney, D. G. *Chem. Rev.* **2005**, *105*, 1563–1602.
(19) Xiaopeng, S.; Que, L. J. *J. Inorg. Biochem.* **2006**, *100*, 421–433.
(20) Groves, J. T. *J. Inorg. Biochem.* **2006**, *100*, 434–447.

Published on Web 09/15/2010

Ru(VI), and Os(VI)[16,17] oxo intermediates or complexes to perform important and chemically challenging synthetic,[8−12] and biological/biomimetic[12−14] reactions. Further, the geometry (*cis* or *trans*) of dioxo metal complexes has a crucial effect on their electronic structure and reactivity.[1−3] For example, N-donor *cis*-dioxo-Ru(VI) and -Os(VI) complexes are generally stronger oxidants than their *trans* isomers and many are active catalysts and electrocatalysts for the oxidation of alcohols, alkenes, aromatic hydrocarbons and alkanes.[21−23] The remainder of the introduction focuses on d^1 *cis*-dioxo metal complexes and their conjugate acids.

The group 6 elements, chromium and molybdenum, form a variety of d^1 *cis*-dioxo complexes. The first *cis*-dioxo-Cr(V) compounds, $[CoCp_2][CrO_2(NRAr)_2]$ (R = $C(CD_3)_2Me$, *t*-Bu; Ar = 2,5-C_6H_3FMe), were prepared by Cummins and co-workers upon reduction of $CrO_2(NRAr)_2$ with cobaltocene in benzene.[24] These pseudo-tetrahedral Cr(V) anions react with electrophiles yielding oxo-Cr(V) complexes. Subsequently, Lay and co-workers reported the in situ generation of *cis*-$[CrO_2(phen)_2]^+$ (phen = 1,10-phenanthroline) by oxidation of *cis*-$[Cr(phen)_2(OH_2)_2]^{3+}$ with aqueous NaOCl.[25] Chromium(V) radicals are implicated in oxidative DNA damage, bacterial mutagenicity, and an increase in micronuclei in mammalian cell lines.[25,26] More recently, groups led by Tsai[27] and Theopold[28] synthesized the β-diketiminate complex, Cr^VO_2(nacnac) (nacnac = $HC(C(Me)NC_6H_3{}^iPr_2)_2^-$), following autoxidation of $[Cr(nacnac)]_2(\mu\text{-}C_7H_8)$ or $[Cr(nacnac)]_2(\mu\text{-}N_2)$, respectively.

Although hundreds of d^0 *cis*-dioxo-Mo(VI) complexes are known only a few *cis*-dioxo-Mo(V) complexes have been reported.[29] Complexes of this type were first prepared in situ by Spence, Wedd, and co-workers upon chemical (SH^-) or electrochemical reduction of the dioxo-Mo(VI) analogues.[30,31] Archetypal *cis,trans*-$[MoO_2(L\text{-}N_2S_2)]^-$ ($L\text{-}N_2S_2{}^{2-}$ = *N,N′*-dimethyl-*N,N′*-bis(2-mercaptophenyl)ethylenediamine) is characterized by a broad, anisotropic electron paramagnetic resonance (EPR) signal at $g = 1.9007$.[30−32] Its conjugate acid, *cis,trans*-MoO(OH)($L\text{-}N_2S_2$), exhibits a proton-split, doublet EPR signal at room temperature ($g = 1.957$, $A_H = 15.1 \times 10^{-4}$ cm^{-1}) but deprotonation of the complex upon freezing produces anisotropic (frozen-glass) EPR spectra that are devoid of proton superhyperfine coupling.[30−32] Interest in the chemical and spectroscopic properties of (hydroxo)oxo-Mo(V) complexes is stimulated by the involvement of such species in the turnover of certain molybdenum enzymes.[33−36] For example, the low pH Mo(V) forms of sulfite oxidases are postulated to contain $[(MPT)Mo^VO(OH)(S\text{-}cys)]^-$ centers formed during the regeneration of the $[(MPT)Mo^{VI}O_2(S\text{-}cys)]^-$ oxidized active site.[33−36]

Many years later, various salts of $[Tp^xMoO_2X]^-$ (Tp^x = hydrotris(3,5-dimethylpyrazol-1-yl)borate (Tp*), hydrotris(3-isopropylpyrazol-1-yl)borate (Tp^{iPr}), hydrotris(3,5-dimethyltriazol-1-yl)borate (Tz*); X = monoanionic ligand) were prepared (in situ)[37−40] and isolated.[41,42] These complexes also exhibit broad anisotropic EPR signals at *g* about 1.92 and protonate to form the conjugate acids, $Tp^xMoO(OH)X$. The latter exhibit doublet EPR signals ($g \sim 1.94$, $A_H \sim 11 \times 10^{-4}$ cm^{-1}) at room temperature but frozen-glass spectra were again devoid of proton superhyperfine coupling. Several (hydroxo)oxo-Mo(V) species were isolated in impure form.[42] The anion of $[CoCp_2][Tz^*MoO_2(SPh)]$ displays a distorted octahedral geometry with Mo═O distances (1.742(9) Å) and an O═Mo═O angle (112.1(4)°) greater than those of the Mo(VI) analogue (1.700(6) Å and 103.9(2)°, respectively).[41,42] These data are consistent with the presence of a semioccupied molecular orbital with significant MoO_2 π^* character. The complexes react with Me_3SiCl to produce $Tp^xMoO(OSiMe_3)X$ (X = Cl^-, Br^-, NCS^-, OPh^-, SPh^-, SCH_2Ph^-).[43]

A number of other *cis*-dioxo-Mo(V) complexes have been reported; interestingly, these exhibit distinctly different physical and spectroscopic properties from the complexes discussed above.[44−46] The EPR spectra of catecholate species resemble those of organic radicals[44,45] while the spectrum of $[CoCp_2][MoO_2(L\text{-}N_2)_2]$ ($L\text{-}N_2$ = $C_4H_3NCHNC_6H_4OSiMe_3$) is sharper and less anisotropic than is typical (vide supra).[46] The $L\text{-}N_2$ complex reacts with triflic acid to form MoO(OH)$(L\text{-}N_2)_2$ but deprotonation upon freezing again prevents the observation of proton superhyperfine coupling at low temperature.[46] To our knowledge, *trans*-dioxo-Mo(V) or authentic *cis*- or *trans*-dioxo-W(V) complexes remain unknown.

The group 7 element, rhenium, also forms a variety of stable d^1 *cis*-dioxo complexes. The first complexes of this

(21) (a) Goldstein, A. S.; Drago, R. S. *J. Chem. Soc., Chem. Commun.* **1991**, 21–22. (b) Goldstein, A. S.; Beer, R. H.; Drago, R. S. *J. Am. Chem. Soc.* **1994**, *116*, 2424–2429. (c) Goldstein, A. S.; Drago, R. S. *J. Chem. Soc., Dalton Trans.* **1996**, 105–110.
(22) Cheng, W.-C.; Yu, W.-Y.; Cheung, K.-K.; Che, C.-M. *J. Chem. Soc., Chem. Commun.* **1994**, 1063–1064.
(23) Wong, K. Y.; Lee, W. O.; Che, C. M.; Anson, F. C. *J. Electronal. Chem. Interface Chem.* **1991**, *319*, 207–216 and references cited therein.
(24) Odom, A. L.; Mindiola, D. J.; Cummins, C. C. *Inorg. Chem.* **1999**, *38*, 3290–3295.
(25) Weeks, C. L.; Levina, A.; Dillon, C. T.; Turner, P.; Fenton, R. R.; Lay, P. A. *Inorg. Chem.* **2004**, *43*, 7844–7856.
(26) Levina, A.; Lay, P. A. *Coord. Chem. Rev.* **2005**, *249*, 281–298.
(27) Tsai, Y.-C.; Wang, P.-Y.; Chen, S.-A.; Chen, J.-M. *J. Am. Chem. Soc.* **2007**, *129*, 8066–8067.
(28) Monillas, W. H.; Yap, G. P. A.; MacAdams, L. A.; Theopold, K. H. *J. Am. Chem. Soc.* **2007**, *129*, 8090–8091.
(29) Young, C. G. In *Comprehensive Coordination Chemistry II*; McCleverty, J. A., Meyer, T. J., Eds.; Elsevier Pergamon: Amsterdam, 2004; Vol. *4*, Chapter 4.7, pp 415−527.
(30) Hinshaw, C. J.; Spence, J. T. *Inorg. Chim. Acta* **1986**, *125*, L17–L21.
(31) Dowerah, D.; Spence, J. T.; Singh, R.; Wedd, A. G.; Wilson, G. L.; Farchione, F.; Enemark, J. H.; Kristofzski, J.; Bruck, M. *J. Am. Chem. Soc.* **1987**, *109*, 5655–5665.
(32) Peng, G.; Nichols, J.; McCullough, E. A., Jr.; Spence, J. T. *Inorg. Chem.* **1994**, *33*, 2857–2864.
(33) Hille, R. *Chem. Rev.* **1996**, *96*, 2757–2816.
(34) Tunney, J. M.; McMaster, J.; Garner, C. D. In *Comprehensive Coordination Chemistry II*; McCleverty, J. A., Meyer, T. J., Eds.; Elsevier Pergamon: Amsterdam, 2004; Vol. *8*, Chapter 8.18, pp 459−477.
(35) Young, C. G. In *Encyclopedia of Inorganic Chemistry 2*; King, R. B., Ed.; Wiley: Chichester, U.K., 2005; Vol. *V*, pp 3321−3340.
(36) Enemark, J. H.; Astashkin, A. V.; Raitsimring, A. M. *Dalton Trans.* **2006**, 3501–3514.
(37) Xiao, Z.; Young, C. G.; Enemark, J. H.; Wedd, A. G. *J. Am. Chem. Soc.* **1992**, *114*, 9194–5.
(38) Xiao, Z.; Bruck, M. A.; Doyle, C.; Enemark, J. H.; Grittini, C.; Gable, R. W.; Wedd, A. G.; Young, C. G. *Inorg. Chem.* **1995**, *34*, 5950–5962.
(39) Laughlin, L. J.; Young, C. G. *Inorg. Chem.* **1996**, *35*, 1050–1058.
(40) Rajapakshe, A.; Snyder, R. A.; Astashkin, A. V.; Bernardson, P.; Evans, D. J.; Young, C. G.; Evans, D. H.; Enemark, J. H. *Inorg. Chim. Acta* **2009**, *362*, 4603–4608.
(41) Xiao, Z.; Gable, R. W.; Wedd, A. G.; Young, C. G. *J. Chem. Soc., Chem. Commun.* **1994**, 1295–1296.
(42) Xiao, Z.; Gable, R. W.; Wedd, A. G.; Young, C. G. *J. Am. Chem. Soc.* **1996**, *118*, 2912–2921.
(43) Xiao, Z.; Bruck, M. A.; Enemark, J. H.; Young, C. G.; Wedd, A. G. *J. Biol. Inorg. Chem.* **1996**, *1*, 415–423.
(44) Lu, X.; Liu, S.; Mao, X.; Bu, X. *J. Mol. Struct.* **2001**, *562*, 89–94.
(45) Lu, X.-M.; Lu, J.-F.; Mao, X.-A. *Chin. J. Chem.* **2002**, *20*, 617–621.
(46) Heinze, K.; Fischer, A. *Eur. J. Inorg. Chem.* **2010**, 1939–1947.

type, namely, $Re^{VI}O_2(aryl)_2$ (aryl = 2,6-dimethylphenyl and 2,4,6-trimethylphenyl), were prepared by Wilkinson and coworkers.[47,48] Later, DuMez and Mayer reported the synthesis and chemical reactions of $TpRe^{VI}O_2X$ (Tp = hydrotrispyrazol-1-ylborate; X = Cl^-, Br^-, I^-).[49] These complexes exhibit octahedral geometries, disproportionate into $TpRe^{VII}O_3$ and $TpRe^{V}OX_2$ and, in contrast to the Cr(V) and Mo(V) complexes above, act as electrophiles rather than nucleophiles.

This paper reports the synthesis of *cis*-dioxo-Mo(VI), *cis*-dioxo-Mo(V) and *cis*-(hydroxo)oxo-Mo(V) complexes that contain Tp^{iPr} and salicylanilide ligands, and are stabilized by an intramolecular hydrogen-bond. The work extends known *cis*-dioxo-Mo(V) chemistry to O-donor ligand systems and increases the number of species to be isolated and fully characterized. The paper focuses on three series of complexes, namely, $Tp^{iPr}Mo^{VI}O_2(2\text{-}OC_6H_4CONHR)$ (**1**−**3** and *N*-methylated **4**), $[CoCp_2][Tp^{iPr}Mo^{V}O_2(2\text{-}OC_6H_4CONHR)]$ (**5**−**7**), and $Tp^{iPr}Mo^{V}O(OH)(2\text{-}OC_6H_4CONHR)$ (**8**−**10**). The H-bond stabilization facilitates brief handling of the dioxo-Mo(V) compounds in air and the quantitative, in situ generation of (hydroxo)oxo-Mo(V) species. Significantly, the (hydroxo)oxo-Mo(V) species persist in frozen glasses, allowing proton superhyperfine coupling to be detected in anisotropic EPR spectra. The research was stimulated by the rarity and potential utility of d^1 *cis*-dioxo-Mo(V) complexes and by the fact that these complexes are precursors for biologically relevant *cis*-(hydroxo)oxo-Mo(V) species.[33−36]

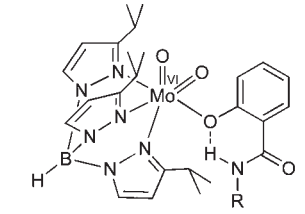

R = Ph (**1**), 4-C_6H_4Cl (**2**), 4-C_6H_4OMe (**3**)

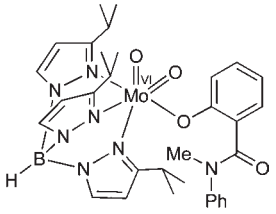

(**4**)

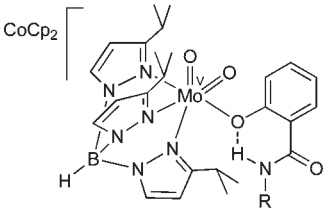

R = Ph (**5**), 4-C_6H_4Cl (**6**), 4-C_6H_4OMe (**7**)

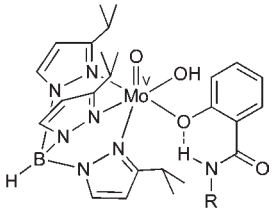

R = Ph (**8**), 4-C_6H_4Cl (**9**), 4-C_6H_4OMe (**10**)

Experimental Section

Materials and Methods. All reactions were performed under an atmosphere of dinitrogen using dried, deoxygenated solvents. The salicylanilide ligands were prepared from salicylic acid and the appropriate aniline using literature methods.[50,51] Samples of $Tp^{iPr}MoO_2(2\text{-}OC_6H_4CONHPh)$ (**1**) were prepared as previously described.[52] Other chemicals were obtained from Aldrich Chemical Co. and were used without purification. Column chromatography was performed using silica gel (mesh size 40−200) columns with dimensions of about 40−60 cm × ∼2.5 cm diameter.

Infrared spectra were recorded on a Bio-Rad FTS 165 FTIR spectrophotometer as pressed KBr disks. Electrospray ionization mass spectrometry (ESI-MS) experiments were carried out using a Micromass Quattro II mass spectrometer using samples dissolved in MeCN. NMR spectra were recorded at room temperature on Varian Unity-Plus 400 MHz or Inova 500 MHz spectrometers. Spectra were referenced to residual solvent peaks (for $CDCl_3$, δ_H 7.24, δ_C 77.0). EPR spectra were recorded on a Bruker ECS 106 EPR spectrometer using 1,2-diphenyl-2-picrylhydrazyl as reference and 10^{-3} M solutions of the compounds in 10:1 THF/CH_3CN mixtures. EPR parameters have been recorded directly from the spectra obtained. Cyclic voltammograms were recorded using a 2 mm glassy carbon working electrode, platinum counter electrode, and a freshly prepared double-jacketed $Ag/AgNO_3$ reference electrode (10 mM $AgNO_3$ in MeCN with 0.1 M $NBu^n_4PF_6$ and clean silver wire), connected to an Autolab Potentiostat operated by the General Purpose Electrochemical System software (version 4.9). Samples were prepared as 1−2 mM solutions in MeCN with 0.1 M $NBu^n_4PF_6$ as supporting electrolyte. Scan rates were varied over the range 10−500 mV s^{-1}. Potentials were referenced against the ferrocene couple, Fc^+/Fc, and are reported relative to SCE. The Fc^+/Fc couple was set to the reported value of +0.400 V versus SCE for acetonitrile/0.1 M $NBu^n_4PF_6$ solutions.[53] Microanalyses were performed by Atlantic Microlab Inc., Norcross, GA.

Syntheses and Characterization Data. *cis*-Dioxo-Mo(VI) Complexes. The procedure below was adopted for the three new $Tp^{iPr}MoO_2(2\text{-}OC_6H_4CONHR)$ complexes (**2**−**4**). Yellow $Tp^{iPr}MoO_2Cl$ (1.00 g, 2 mmol) and the appropriate ligand (5 mmol) were dissolved in CH_2Cl_2 (30 mL) in a Schlenk flask, and then NEt_3 (3−4 mL, ca. 20−30 mmol) was added. The reaction mixture was stirred vigorously for 1.5 days and then reduced to dryness by rotary evaporation. The residue was purified by column chromatography on silica gel using 2:1 CH_2Cl_2/hexane as solvent (1:1 CH_2Cl_2/hexane, for **4**). The complex usually eluted as the third or fourth band (yellow, orange, or red), after unreacted $Tp^{iPr}MoO_2Cl$, excess parent phenol, and unidentified brown products. The isolated fraction was reduced to dryness and then treated with methanol and refrigerated to yield crystals. The compounds were recrystallized from dichloromethane/hexane or dichloromethane/methanol mixtures.

R = 4-C_6H_4Cl (2). Yield 1.02 g (71%). Anal. Calcd for $C_{31}H_{37}BMoN_7O_4Cl$: C, 52.15; H, 5.22; N, 13.74. Found: C, 51.89; H, 5.40; N, 13.82. IR (KBr, cm^{-1}): ν(NH) 3310 s, 3144 w, 3120 w, 3067 w, 2972 s, 2929 m, 2871 w, ν(BH) 2501 m and 2459 sh-w, ν(C=O) 1676 s, 1592 s, 1536 s, ν(CN) 1506 s, 1493 s, 1472 m, 1447 m, 1401 m, 1387 m, 1365 m, 1317 m, 1291 m, 1251 m, 1217 s, 1197 s, 1160 w, 1104 w, 1094 w, 1083 w, 1072 m, 1050 s, 1025 w, 1013 w, $\nu(MoO_2)$ 937 s and 904 vs, 858 w, 832 w, 820 w, 795 w, 782 m, 759 m, 730 s, 713 w, 697 w, 676 w, 646 w, 630 w, 620 w, 503 w, 477 w, 425 w. ^1H NMR ($CDCl_3$): δ_H 10.01 (1H, br s), 8.28 (1H, dd, J = 7.8, 2.0 Hz), 7.72 (1H, d, J = 2.4 Hz), 7.60−7.65 (3H, overlapping peaks), 7.48 (1H, d, J = 8.0 Hz), 7.17 (1H, t, J = 7.6 Hz), 6.90 (2H, d, J = 8.8 Hz), 6.24 (2H, d, J = 8.8 Hz), 6.20 (1H, d, J = 2.4 Hz), 5.98 (2H, d, J = 2.4 Hz), 4.21 (1H, sept, J = 6.8 Hz), 3.21 (2H, sept, J = 6.8 Hz), 1.28 (6H, d, J = 6.8 Hz), 1.04 (6H, d, J = 6.8 Hz), 0.87 (6H, d, J = 6.8 Hz). $^{13}C\{^1H\}$ NMR ($CDCl_3$): δ_C 165.5, 163.0, 162.5, 138.2,

(47) Stravropoulos, P.; Edwards, P. G.; Behling, T.; Wilkinson, G.; Motevalli, M.; Hursthouse, M. B. *J. Chem. Soc., Dalton Trans.* **1987**, 169–175.
(48) Longley, C. J.; Savage, P. D.; Wilkinson, G.; Hussain, B.; Hursthouse, M. B. *Polyhedron* **1988**, *7*, 1079–1088.
(49) DuMez, D. D.; Mayer, J. M. *Inorg. Chem.* **1998**, *37*, 445–453.
(50) Waisser, K.; Hladuvkova, J.; Kunes, J.; Kubicova, L.; Klimesova, V.; Karajannis, P.; Kaustova, J. *Chem. Pap.* **2001**, *55*, 121–129.
(51) Waisser, K.; Perina, M.; Holy, P.; Pour, M.; Bures, O.; Kunes, J.; Klimesova, V.; Buchta, V.; Kubanova, P.; Kaustova, J. *Archiv. Pharm.* **2003**, *336*, 322–335.
(52) Hill, L. M. R.; Taylor, M. K.; Ng, V. W. L.; Young, C. G. *Inorg. Chem.* **2008**, *47*, 1044–1052.
(53) Connelly, N. G.; Gieger, W. E. *Chem. Rev.* **1996**, *96*, 877–910.

136.7, 136.1, 134.2, 131.4, 128.2, 127.8, 122.1, 121.5, 120.8, 120.0, 102.9, 102.8, 28.4, 27.4, 24.4, 22.9, 22.1. ESI-MS: *m*/*z* 716.5 $[M + H]^+$, 606.4 $[M - C_6H_9N_2]^+$. Cyclic voltammetry: $E_{1/2} = -0.565$ V (quasi-reversible, Mo^{VI}/Mo^{V}).

R = 4-C_6H_4OMe (3). Yield 0.60 g (43%). Anal. Calcd for $C_{31}H_{38}BMoN_7O_4$: C, 54.17; H, 5.68; N, 13.82. Found: C, 54.17; H, 5.69; N, 13.89. IR (KBr, cm^{-1}): ν(NH) 3311 s, 3134 w, 3118 w, 3072 w, 2970 s, 2928 m, 2870 w, 2833 w, ν(BH) 2499 m and 2459 sh-w, ν(C=O) 1660 s, 1619 w, 1602 w, 1593 m, 1540 m, ν(CN) 1509 vs, 1471 m, 1447 m, 1413 w, 1400 m, 1387 m, 1365 m, 1321 w, 1292 m, 1283 m, 1243 s, 1219 s, 1193 s, 1158 w, 1128 w, 1104 w, 1084 m, 1071 m, 1049 s, 1026 m, $\nu(MoO_2)$ 936 s and 903 vs, 862 w, 845 w, 828 w, 795 w, 781 m, 759 m, 730 s, 711 w, 680 w, 664 w, 633 w, 621 m, 568 w, 521 w, 472 w, 452 w, 425 w. ^{1}H NMR ($CDCl_3$): δ_H 9.81 (1H, br s), 8.29 (1H, d, J = 7.6 Hz), 7.70 (1H, d, J = 2.4 Hz), 7.50−7.65 (3H, overlapping peaks), 7.45 (1H, d, J = 8.0 Hz), 7.16 (1H, t, J = 7.6 Hz), 6.48 (2H, d, J = 8.8 Hz), 6.23 (2H, d, J = 8.8 Hz), 6.19 (1H, d, J = 2.4 Hz), 5.97 (2H, d, J = 2.4 Hz), 4.22 (1H, sept, J = 6.8 Hz), 3.71 (3H, s), 3.22 (2H, sept, J = 6.8 Hz), 1.28 (6H, d, J = 6.8 Hz), 1.04 (6H, d, J = 6.8 Hz), 0.88 (6H, d, J = 6.8 Hz). $^{13}C\{^1H\}$ NMR ($CDCl_3$): δ_C 165.5, 165.4, 162.5, 162.4, 155.3, 138.1, 136.0, 133.8, 131.5, 131.4, 122.0, 121.9, 120.7, 120.2, 113.2, 102.8, 102.7, 55.3, 28.4, 27.4, 24.5, 22.9, 22.1. ESI-MS: *m*/*z* 712.5 $[M + H]^+$, 602.4 $[M - C_6H_9N_2]^+$. Cyclic voltammetry: $E_{1/2} = -0.594$ V (quasi-reversible, Mo^{VI}/Mo^{V}).

$Tp^{iPr}MoO_2${2-OC_6H_4CON(Me)Ph} (4). Yield 0.70 g (50%). Anal. Calcd for $C_{32}H_{40}BMoN_7O_4$: C, 55.42; H, 5.81; N, 14.14. Found: C, 55.30; H, 5.40; N, 14.15. IR (KBr, cm^{-1}): 3149 w, 3110 w, 3065 w, 2974 s, 2926 m, 2870 m, ν(BH) 2486 m and 2460 sh-w, ν(C=O) 1631 s, 1596 s, 1567 w, ν(CN) 1507 s, 1497 s, 1474 m, 1459 m, 1446 s, 1421 w, 1401 m, 1385 s, 1371 s, 1306 m, 1289 m, 1258 s, 1244 s, 1201 s, 1192 s, 1163 w, 1158 w, 1119 w, 1106 w, 1083 m, 1070 s, 1050 s, 1028 w, 1000 w, $\nu(MoO_2)$ 931 s and 903 vs, 868 m, 837 w, 821 w, 796 m, 777 m, 763 m, 752 s, 733 s, 722 w, 714 w, 700 m, 660 m, 628 m, 587 m, 544 w, 514 w, 477 m, 424 w. ^{1}H NMR ($CDCl_3$): δ_H 7.55−7.60 (3H, overlapping peaks), 7.21 (5H, br s), 7.10 (1H, br s), 6.63 (2H, br d), 6.11 (1H, d, J = 2.4 Hz), 5.95 (2H, br s), 4.98 (1H, br s), 4.46 (1H, br s), 3.59 (3H, s, NCH_3), 3.24 (2H, br s), 1.27 (6H, d, J = 6.8 Hz), 1.09 (6H, d, J = 6.8 Hz), 0.47 (6H, br s). $^{13}C\{^1H\}$ NMR ($CDCl_3$): δ_C 168.5, 165.0, 164.9, 157.5, 137.2, 135.4, 129.4, 129.1, 128.6, 128.3, 127.0, 126.0, 117.9, 102.3, 101.8, 37.8, 28.2, 27.0, 24.7, 23.2, 21.9. ESI-MS: *m*/*z* 696.7 $[M + H]^+$, 586.6 $[M - C_6H_9N_2]^+$. Cyclic voltammetry: $E_{1/2} = -0.834$ V (quasi-reversible, Mo^{VI}/Mo^{V}).

***cis*-Dioxo-Mo(V) Compounds.** The general procedure that follows was adopted for the synthesis of the $[CoCp_2][Tp^{iPr}MoO_2(2\text{-}OC_6H_4CONHR)]$ complexes. A solution of cobaltocene (0.30 g, 1.59 mmol) in 10 mL of dry deoxygenated toluene was cannula-filtered into a stirred solution of $Tp^{iPr}MoO_2(2\text{-}OC_6H_4CONHR)$ (1.0 mmol); the mixture was stirred for 30 min. The resultant emerald green microcrystalline solid was collected by filtration. The solid was washed with dry toluene (5 mL) under nitrogen and dried in vacuo. The complexes may be further purified via recrystallization from either a mixture of acetonitrile/diethyl ether or dichloromethane/hexane.

R = Ph (5). Yield: 0.78 g (90%). Anal. Calcd for $C_{41}H_{48}BCoMoN_7O_4$: C, 56.69; H, 5.57; N, 11.29. Found: C, 56.49; H, 5.74; N, 11.30. IR (KBr, cm^{-1}): ν(N−H) 3316 w, br, 3107 m, 3087 m, 3051 m, 3024 m, 2966 m, 2927 m, 2868 m, ν(BH) 2472 w and 2439 w, ν(C=O) 1651 vs, 1593 s, 1537 s, ν(CN) 1508 s, 1467 s, 1452 s, 1415 m, 1398 m, 1384 m, 1360 m, 1325 s, 1299 w, 1287 w, 1261 m, 1236 m, 1193 s, 1153 m, 1123 w, 1104 m, 1069 m, 1044 s, 1016 m, $\nu_s(MoO_2)$ 894 m, 875 m, 857 m, 829 m, 815 m, $\nu_{as}(MoO_2)$ 791 s, 773 vs, 756 s, 732 s, 695 m, 665 w, 628 w, 607 w, 580 w, 567 vw, 541 vw, 512 w, 504 vw, $\nu([CoCp_2]^+)$ 460 m, 425 w. EPR (THF/MeCN, 298 K): g_{iso} 1.908, $A(^{95,97}Mo)$ 45.15×10^{-4} cm^{-1}. ESI-MS: *m*/*z* 682.3 $[M]^-$. Cyclic voltammetry: $E_{1/2} = -0.598$ V (reversible, Mo^{VI}/Mo^{V}); $E_{1/2} = -0.94$ V (reversible, $[CoCp_2]^+/CoCp_2$); $E_{1/2} = -1.88$ V (reversible, $CoCp_2/[CoCp_2]^-$).

R = 4-C_6H_4Cl (6). Yield: 0.77 g (85%). Anal. Calcd for $C_{41}H_{47}BClCoMoN_7O_4$: C, 54.53; H, 5.25; N, 10.86. Found: C, 54.81; H, 5.22; N, 10.82. IR (KBr, cm^{-1}): ν(N−H) 3306 w, br, 3107 m, 3062 m, 3018 m, 2966 s, 2927 m, 2868 m, ν(BH) 2486 w and 2449 w, ν(C=O) 1656 vs, 1590 vs, 1535 vs, ν(CN) 1508 vs, 1493 vs, 1466 vs, 1452 vs, 1416 s, 1400 s, 1384 s, 1361 m, 1324 s, 1293 m, 1260 m, 1236 m, 1193 vs, 1150 m, 1124 w, 1104 m, 1090 m, 1069 m, 1043 vs, 1013 m, $\nu_s(MoO_2)$ 896 m, 877 s, 861 s, 832 s, $\nu_{as}(MoO_2)$ 792 vs, 775 vs, 733 vs, 718 w, 697 w, 628 w, 603 w, 578 w, 542 w, 511 w, $\nu([CoCp_2]^+)$ 460 m, 427 m. EPR (THF/toluene, 298 K): g_{iso} 1.907, $A(^{95,97}Mo)$ 45.58×10^{-4} cm^{-1}. ESI-MS: *m*/*z* 715.2 $[M]^-$. Cyclic voltammetry: $E_{1/2} = -0.565$ V (reversible, Mo^{VI}/Mo^{V}); $E_{1/2} = -0.94$ V (reversible, $[CoCp_2]^+/CoCp_2$); $E_{1/2} = -1.88$ V (reversible, $CoCp_2/[CoCp_2]^-$).

R = 4-C_6H_4OMe (7). Yield: 0.72 g (80%). Anal. Calcd for $C_{42}H_{50}BCoMoN_7O_5$: C, 56.14; H, 5.61; N, 10.91. Found: C, 56.42; H, 5.69; N, 10.78. IR (KBr, cm^{-1}): ν(N−H) 3319 w, br, 3115 m, 3102 m, 3066 m, 3032 m, 2997 m, 2967 m, 2927 m, 2868 m, 2832 w, ν(BH) 2498 w and 2454 w, ν(C=O) 1644 vs, 1592 m, 1541 s, ν(CN) 1510 vs, 1467 s, 1450 s, 1416 s, 1395 m, 1384 s, 1362 m, 1335 w, 1305 m, 1289 m, 1257 m, 1242 vs, 1194 s, 1185 s, sh, 1151 m, 1123 w, 1107 m, 1070 m, 1064 m, 1044 s, 1029 m, $\nu_s(MoO_2)$ 895 m, 873 s, 863 s, 842 m, 828 s, $\nu_{as}(MoO_2)$ 792 s, 779 vs, 769 vs, 732 s, 717 m, 696 w, 654 vw, 625 w, 606 w, 578 w, 541 w, 523 w, 504 vw, $\nu([CoCp_2]^+)$ 464 m, 428 w. EPR (THF/toluene, 298 K): g_{iso} 1.907, $A(^{95,97}Mo)$ 44.58×10^{-4} cm^{-1}. ESI-MS: *m*/*z* 711.4 $[M]^-$. Cyclic voltammetry: $E_{1/2} = -0.594$ V (reversible, Mo^{VI}/Mo^{V}); $E_{1/2} = -0.94$ V (reversible, $[CoCp_2]^+/CoCp_2$); $E_{1/2} = -1.88$ V (reversible, $CoCp_2/[CoCp_2]^-$).

Protonation of $[CoCp_2][Tp^{iPr}MoO_2(2\text{-}OC_6H_4CONHR)]$ (in situ EPR Experiments). The following procedure was adopted for all three derivatives: Samples of **5**, **6**, or **7** (ca. 9 mg, $\sim 1 \times 10^{-5}$ mol) and lutidinium tetrafluoroborate (ca. 3 mg, $\sim 1.5 \times 10^{-5}$ mol) were dissolved in 1 mL of dry deoxygenated 1:1 toluene/THF mixture. An immediate color change from pale green to brown-yellow was observed, together with a precipitate of yellow $[CoCp_2]$-BF_4. The mixture was then filtered, and the filtrate introduced into an anaerobic EPR tube for analysis. The *cis*-(hydroxo)oxo-Mo(V) complexes, **8** (R = Ph), **9** (R = 4-C_6H_4Cl), and **10** (R = 4-C_6H_4-OMe), were characterized by EPR spectroscopy (vide infra). To date, all attempts to isolate the complexes have led to the precipitation of mixtures contaminated with the conjugate base and trace molybdenyl species.

X-ray Crystallography. Crystal data are provided in Table 1. Crystals were coated in mineral oil and mounted on glass fibers. Crystals of **1** and **3** were obtained from slow evaporation of an ethyl acetate solution of **1** and slow diffusion of hexane into a toluene solution of **3**. Crystals of **2** and **4** were obtained from slow diffusion of hexane into dichloromethane solutions of the complexes. All the *cis*-dioxo-Mo(V) crystals (**5**−**7**) were grown by slow diffusion of ether into acetonitrile solutions of the complexes. Data for the X-ray structure determinations described in this paper were collected on a Bruker CCD area detector at 130 K using Mo Kα radiation (0.71073 Å) for complexes **2** and **5**, and an Oxford XCalibur diffractometer at 130 K using Cu Kα radiation (1.54184 Å) for complexes **1**, **3**, **4**, **6**, and **7**. Cell parameters for **2** and **5** were acquired by the SMART software package, and data reduction was performed using SAINT; the cell parameters and data reduction for complexes **1**, **3**, **4**, **6**, and **7** were performed on the Chrysalis software. Structures were solved by direct methods (SHELXS-97[54]) and refined using full-matrix least-squares on F^2 (SHELXL-97[55]).

(54) Sheldrick, G. M. *SHELXS-97 Program for Crystal Structure Solution*; University of Göttingen: Göttingen, Germany, 1997.
(55) Sheldrick, G. M. *SHELXL-97 Program for Crystal Structure Refinement*, University of Göttingen: Göttingen, Germany, 1997.

Table 1. Crystallographic Data

parameter	**1**·H_2O	**2**	**3**	**4**	**5**·2CH_3CN·1/2$C_4H_{10}O$	**6**·CH_3CN	**7**·CH_3CN
formula	$C_{31}H_{40}BMoN_7O_5$	$C_{62}H_{74}B_2Cl_2Mo_2N_{14}O_8$	$C_{32}H_{40}BMoN_7O_5$	$C_{32}H_{40}BMoN_7O_4$	$C_{88}H_{107}B_2Co_2Mo_2N_{16}O_{8.5}$	$C_{43}H_{50}BClCoMoN_8O_4$	$C_{44}H_{53}BCoMoN_8O_5$
formula mass	697.45	1427.75	709.46	693.46	928.13	943.03	939.62
crystal system	monoclinic	triclinic	monoclinic	triclinic	triclinic	monoclinic	triclinic
space group	$P2_1/c$	$P\bar{1}$	$P2_1/c$	$P\bar{1}$	$P\bar{1}$	$C2/c$	$P\bar{1}$
a, Å	16.96030(10)	12.287(5)	8.5817(2)	8.7355(8)	11.3967(12)	24.1593(6)	10.9831(11)
b, Å	10.55090(10)	15.054(5)	13.2801(3)	11.2816(9)	12.6907(13)	11.0661(2)	12.7023(7)
c, Å	18.2873(2)	18.663(5)	29.2857(5)	17.2653(12)	17.3524(18)	34.8794(2)	17.3313(12)
α, deg	90	96.058(5)	90	92.468(6)	83.610(2)	90	86.255(5)
β, deg	90.2490(10)	95.106(5)	94.431(2)	97.569(7)	82.018(2)	113.643(2)	81.535(7)
γ, deg	90	98.953(5)	90	103.852(8)	64.617(2)	90	65.337(7)
V, Å^3	3272.42(5)	3371(2)	3327.59(12)	1632.7(2)	2241.7(4)	8542.3(3)	2173.4(3)
Z	4	2	4	2	2	8	2
T, K	130(2)	130(2)	130(2)	130(2)	130(2)	130(2)	130(2)
ρ, gcm^{-3}	1.416	1.406	1.416	1.411	1.375	1.467	1.436
μ, cm^{-1}	3.69	5.14	3.64	3.67	7.00	7.97	5.792
data	13544	17928	12857	10520	14137	14163	13781
unique data	5813	11685	6495	6243	9815	8502	7168
R_1 [$I > 2\sigma(I)$][a]	0.0590	0.0367	0.0470	0.0466	0.0528	0.0405	0.0506
wR_2 (F^2, all data)[b]	0.1499	0.0918	0.1226	0.1294	0.1459	0.1064	0.1473
GoF	1.169	1.028	1.188	1.118	1.075	1.066	1.089

[a] $R_1 = \sum||F_o| - |F_c||/\sum|F_o|$. [b] $wR_2 = \{[\sum w(F_o^2 - F_c^2)^2/\sum(wF_o^2)^2]\}^{1/2}$.

Molecular diagrams were generated using ORTEP-3[56] and the Mercury[57,58] software available from the Cambridge Crystallographic Data Centre. All non-hydrogen atoms were included in difference maps and anisotropic parameters were employed. Hydrogen atoms were included in calculated positions, but this was not possible for the water and disordered acetonitrile molecules in the lattices of **1** and **5**, respectively. All ORTEP projections have been drawn at the 30% probability level with all the H atoms, except N*H*, and lattice solvent molecules omitted for clarity The numbering schemes for the pyrazole rings containing N(21) and N(31) follow those shown for the rings containing N(11).

Results and Discussion

Synthesis and Characterization of *cis*-Dioxo-Mo(VI) Complexes. The red−orange, *cis*-dioxo-Mo(VI) complexes, **1**−**4**, were synthesized by the metathesis reaction shown in eq 1. Optimized syntheses are reported; longer reaction times or gentle heating only result in decomposition. The complexes are air stable as solids and in dry, non-aqueous solutions (the presence of water leads to *very slow* decomposition). Correct microanalyses were obtained for all complexes, and the parent ions $[M+H]^+$ were detected by positive-ion ESI-MS.

$$Tp^{iPr}MoO_2Cl + HOC_6H_4CON(H/Me)R + NEt_3 \rightarrow \mathbf{1-4} + NEt_3HCl \quad (1)$$

The infrared spectra of the complexes exhibited bands at about 935 and 900 cm^{-1} assignable to the symmetric and antisymmetric stretching modes, respectively, of the *cis*-$Mo^{VI}O_2$ moiety; the positions and intensities of these bands were consistent with literature values for related complexes.[52] Bands characteristic of the Tp^{iPr} (ν(BH) 2521−2458 cm^{-1}, ν(CN) ca. 1507 cm^{-1}) and phenolate (ν(CO) ca. 1570 cm^{-1} and $\nu(CC)_{ring}$ ca. 1260 cm^{-1}) ligands were also present.[52] Monosubstitution of the phenolate ligands is reflected by the bands associated with the CH out-of-plane bending bands in the 900−680 cm^{-1} region.[59] The carbonyl functional groups give rise to characteristic bands at about 1631−1774 cm^{-1}, close to those of the corresponding free ligands, consistent with noncoordinating carbonyl groups. Finally, complexes **1**−**3** exhibit N−H stretching bands at about 3310 cm^{-1}, the relatively low intensity of these bands being indicative of H-bonding to the phenolate oxygen (confirmed via X-ray crystallography, vide infra).

The NMR spectra of the complexes were consistent with molecular C_s symmetry in solution. The Tp^{iPr} ligands are represented by three doublet methyl resonances of equal intensity (six protons each), two septet isopropyl C*H* resonances with an intensity ratio of 2:1, and two sets of doublet pyrazole ring resonances, each with a 2:1 intensity ratio. Resonances assignable to the protons of the phenolate ligand were also present, the NH resonance being broad and indicative of the presence of H-bonding. Complex **4** exhibited broad, room temperature NMR resonances indicative of fluxionality (also a feature of related complexes[52]). Complexes **1**−**3** are nonfluxional; this behavior provides evidence for the persistence of the intramolecular H-bond revealed by X-ray crystallography (vide infra) in solution.

Electrochemistry. The electrochemical properties of the *cis*-dioxo-Mo(VI) complexes in acetonitrile were investigated by cyclic voltammetry (see Experimental Section). All complexes exhibited a single, quasi-reversible, one-electron reduction (eq 2) in the potential range −0.834 to −0.565 V versus SCE. No other electrochemical processes were observed.

$$\mathbf{1-4} + e^- \rightarrow [Tp^{iPr}MoO_2\{2\text{-}OC_6H_4CON(H/Me)R\}]^- \quad (2)$$

(56) Farrugia, L. J. *J. Appl. Crystallogr.* **1997**, *30*, 565.
(57) Bruno, I. J.; Cole, J. C.; Edgington, P. R.; Kessler, M.; Macrae, C. F.; McCabe, P.; Pearson, J.; Taylor, R. *Acta Crystallogr., Sect. B* **2002**, *58*, 389–397.
(58) Macrae, C. F.; Edgington, P. R.; McCabe, P.; Pidcock, E.; Shields, G. P.; Taylor, R.; Towler, M.; van de Streek, J. *J. Appl. Crystallogr.* **2006**, *39*, 453–457.
(59) Williams, D. H.; Fleming, I. *Spectroscopic Methods in Organic Chemistry*, 5th ed.; McGraw-Hill: London, 1995.

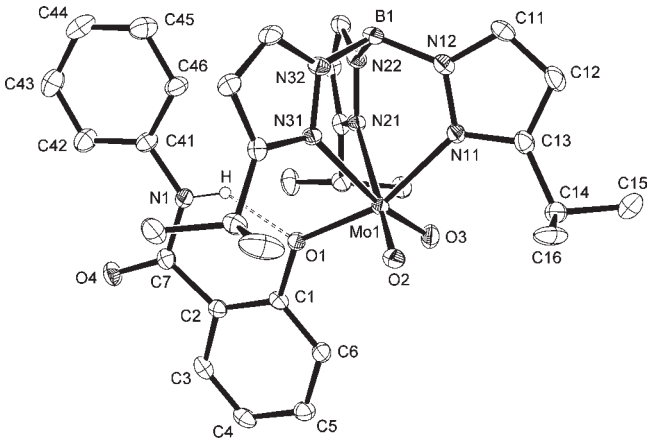

Figure 1. ORTEP projection for **1** (see Experimental Section for details).

The salicylanilide complexes (**1**−**3**) exhibit more positive reduction potentials than other dioxo-Mo(VI) phenolate complexes of Tp^{iPr} (including **4**).[52,60,61] This difference is likely to arise from inductive effects associated with the $NH\cdots O_{phenolate}$ H-bond. Specifically, the interaction stabilizes the Mo-based LUMO facilitating reduction of Mo(VI) to Mo(V). Sengar et al.[62] have reported a similar effect in the electrochemical behavior of the thiophenolate complexes, $Tp^*MoO_2(2\text{-}SC_6H_4CONHR)$. Indeed, the incorporation of H-bonding amido functionalities into the title complexes shifts their potentials into the range reported for the thiophenolate complexes described by Sengar et al.[62] The potentials and reversibility of the Mo(VI/V) electrochemical reductions indicated that stable dioxo-Mo(V) salicylanilide complexes should be chemically accessible upon reduction of the Mo(VI) complexes by cobaltocene (vide infra).[53]

Crystal Structures. The crystal structures of **1**−**4** were determined by X-ray crystallography and representative structures are shown in Figures 1 and 2 (see also: Supporting Information). Crystallographic data and selected bond distances and angles are presented in Tables 1 and 2, respectively. All complexes feature mutually *cis* oxo and O-donor phenolate ligands, a tridentate *fac*-Tp^{iPr} ligand, and a distorted octahedral coordination geometry at Mo(1). The metrical parameters (Table 2) are consistent with those determined for related complexes[52] and will not be discussed in detail.

The phenolate ligands and their phenylamido groups adopt two different conformations in complexes **1**−**4**. In **1**−**3**, the phenolate ring is proximal to the terminal oxo ligands and the amido group is directed toward a cleft in the Tp^{iPr} ligand and is nestled between the two isopropyl groups on the pyrazolyl rings *trans* to the oxo ligands. In these complexes, the Mo(1)−O(1)−C(1) angles range from 131−136°, C(1) lies beneath the MoO_2 plane, and the 6-C*H* proton projects toward and makes close contact with the oxo ligands ($O\cdots HC$ ca. 2.8 Å) (see Figure 1). In complex **4**, the phenolate ring lies in the Tp^{iPr} ligand cleft, and the amido group projects toward the oxo groups

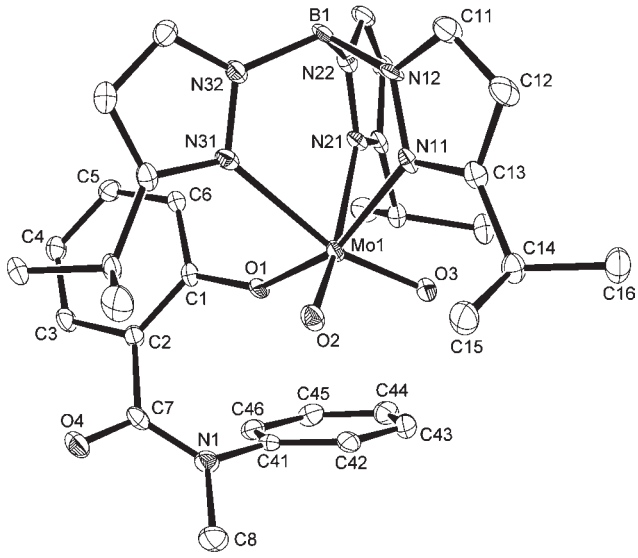

Figure 2. ORTEP projection for **4** (see Experimental Section for details).

(Figure 2). The complex exhibits an Mo(1)−O(1)−C(1) angle of 147.3(2)°, and the C(1) atom points away from the oxo ligands and is positioned beneath the Mo(1), N(21),N(31) plane. The phenolate ring lies close to the pseudo-mirror plane defined by Mo(1), B(1), and N(11) in **1** but is displaced considerably from this plane in **2**, **3**, and **4**. Previously reported derivatives also adopt the two conformations described above.[52]

The amido N(1)−H group of **1**−**3** is H-bonded to the phenolate oxygen O(1) forming a six-membered ring involving these atoms and C(1), C(2), and C(7). The $N(1)\cdots O(1)$ distances range from 2.641(3)−2.680(5) Å while the $H\cdots O$ distances range from 1.894(2)−2.053(2) Å; both values are indicative of strong H-bonding.[63,64] The $N(1)-H\cdots O(1)$ angles range from 124.7(2)−141.7(2)°, a substantial deviation from the ideal angle of 180°; this deviation may be attributed to incorporation of the H-bond into a rigid, six-membered ring.[65−67] A complete listing of the $N(1)-H\cdots O(1)$ bond lengths and angles is included in the Supporting Information. There is no intramolecular H-bond present in **4**.

Synthesis and Characterization of *cis*-Dioxo-Mo(V) Compounds. Pale green microcrystals of the *cis*-dioxo-Mo(V) compounds, **5**−**7**, were precipitated in high yield upon cobaltocene reduction of **1**−**3**, respectively (eq 3). Complex **4** was not cleanly or completely reduced by cobaltocene (nor were related, functionalized dioxo-Mo(VI) phenolate complexes[52]).

$$Tp^{iPr}MoO_2(2\text{-}OC_6H_4CONHR) + CoCp_2 \rightarrow \mathbf{5}-\mathbf{7} \quad (3)$$

Compounds **5**−**7** are air sensitive and slowly react with dioxygen to reform their Mo(VI) precursors; as solids, they can be handled in air for long periods without significant decomposition. They are soluble in acetonitrile and chlorinated solvents but insoluble in non-polar solvents

(60) Millar, A. J.; Doonan, C. J.; Laughlin, L. J.; Tiekink, E. R. T.; Young, C. G. *Inorg. Chim. Acta* **2002**, *337*, 393–406.
(61) Doonan, C. J.; Millar, A. J.; Nielsen, D. J.; Young, C. G. *Inorg. Chem.* **2005**, *44*, 4506–4514.
(62) Sengar, R. S.; Miller, J. J.; Basu, P. *Dalton Trans.* **2008**, 2569–2577.
(63) Desiraju, G. R. *Acc. Chem. Res.* **1991**, *24*, 290–296.
(64) Desiraju, G. R. *Acc. Chem. Res.* **1996**, *29*, 441–449.
(65) Steiner, T. *Chem. Commun.* **1997**, 727–734.
(66) Jeffrey, G. A. *J. Mol. Struct.* **1999**, *485*−*6*, 293–298.
(67) Steiner, T. *Crystallogr. Rev.* **2003**, *9*, 177–228.

Table 2. Selected Bond Distances (Å) and Angles (deg)

parameter	1	2[a]	2[a]	3	4	5	6	7
Mo(1)−O(1)	1.965(4)	1.953(2)	1.941(2)	1.938(3)	1.904(2)	2.054(2)	2.0793(15)	2.062(3)
Mo(1)−O(2)	1.691(5)	1.685(2)	1.697(2)	1.696(3)	1.703(3)	1.732(2)	1.7354(16)	1.724(4)
Mo(1)−O(3)	1.684(4)	1.702(2)	1.694(2)	1.699(3)	1.696(3)	1.741(2)	1.7376(16)	1.759(4)
Mo(1)−N(11)	2.170(5)	2.170(3)	2.176(2)	2.199(3)	2.204(3)	2.203(3)	2.2044(19)	2.207(4)
Mo(1)−N(21)	2.302(5)	2.308(2)	2.324(2)	2.337(4)	2.312(3)	2.376(3)	2.369(2)	2.393(4)
Mo(1)−N(31)	2.319(5)	2.325(2)	2.316(3)	2.329(4)	2.334(3)	2.312(3)	2.3767(19)	2.322(4)
C(1)−O(1) (phenoxy)	1.354(7)	1.363(3)	1.356(3)	1.368(5)	1.361(4)	1.339(4)	1.331(3)	1.335(6)
C(7)−O(4) (carbonyl)	1.234(8)	1.219(3)	1.225(4)	1.235(6)	1.232(5)	1.223(5)	1.230(3)	1.241(6)
Mo(1)−O(1)−C(1)	132.9(4)	131.73(18)	135.58(18)	133.7(3)	147.3(2)	132.7(2)	131.14(14)	134.1(3)
O(1)−Mo(1)−O(2)	99.7(2)	99.13(9)	100.43(10)	101.58(15)	102.11(11)	96.57(11)	93.96(7)	96.92(15)
O(1)−Mo(1)−O(3)	99.8(2)	99.63(10)	102.98(9)	100.20(14)	101.15(12)	94.91(12)	96.16(7)	95.32(16)
O(2)−Mo(1)−O(3)	103.1(2)	102.86(10)	102.60(10)	103.09(16)	102.97(13)	112.75(12)	112.80(8)	111.77(17)
N(11)−Mo(1)−O(1)	160.10(19)	159.92(8)	155.62(9)	160.09(14)	159.92(11)	166.22(10)	166.42(7)	164.80(15)
N(11)−Mo(1)−O(2)	92.0(2)	94.26(10)	94.15(10)	91.09(15)	90.45(12)	91.60(11)	90.85(7)	93.24(16)
N(11)−Mo(1)−O(3)	93.1(2)	91.83(10)	92.66(10)	91.65(15)	91.04(12)	92.12(12)	93.66(7)	91.34(17)
N(21)−Mo(1)−O(1)	84.34(18)	82.55(9)	80.41(9)	83.97(14)	85.41(11)	84.79(11)	85.95(6)	84.12(14)
N(21)−Mo(1)−O(2)	165.5(2)	167.13(10)	169.43(9)	165.56(14)	163.66(11)	161.97(12)	161.98(7)	162.07(17)
N(21)−Mo(1)−O(3)	89.8(2)	89.35(9)	87.38(9)	88.83(14)	89.56(12)	84.95(11)	85.08(7)	85.87(16)
N(31)−Mo(1)−O(1)	83.54(18)	83.87(9)	83.02(8)	84.71(13)	86.64(10)	85.59(10)	86.63(6)	84.20(15)
N(31)−Mo(1)−O(2)	88.7(2)	89.59(9)	89.60(10)	89.71(15)	86.68(12)	86.60(12)	86.53(7)	86.85(17)
N(31)−Mo(1)−O(3)	166.9(2)	166.25(9)	165.00(10)	164.92(14)	165.87(12)	160.39(11)	160.13(7)	161.25(16)
N(11)−Mo(1)−N(21)	80.62(19)	81.14(9)	81.77(9)	80.31(14)	78.72(11)	84.04(11)	85.57(7)	82.75(15)
N(11)−Mo(1)−N(31)	80.64(18)	81.32(9)	77.61(9)	80.03(14)	78.43(10)	83.83(10)	80.99(7)	85.11(15)
N(21)−Mo(1)−N(31)	77.86(19)	77.87(9)	80.02(9)	77.44(13)	79.24(11)	75.56(11)	75.47(6)	75.42(15)
Mo(1)−(O_3)[b]	0.8042(27)	0.8121(12)	0.7798(12)	0.7882(18)	0.7767(15)	0.826(16)	0.8131(10)	0.8090(22)
Mo(1)−(N_3)[c]	1.5189(30)	1.5129(15)	1.5234(15)	1.5441(21)	1.5519(18)	1.5080(18)	1.5280(11)	1.5139(25)
Mo(1)−equatorial[d]	0.0921(24)	0.0745(12)	0.0935(11)	0.1215(18)	0.1566(13)	0.0478(14)	0.0495(9)	0.0399(19)
Ph/(Mo(1),N(11),B)[e]	5.99(43)	13.00(18)	19.64(16)	19.64(16)	31.78(19)	17.61(19)	30.78(13)	19.88(25)

[a] Parameters for crystallographically unique molecules A and B. [b] Displacement of Mo atom from the plane defined by O(1)−O(3) (Å). [c] Displacement of Mo atom from the plane defined by N(11), N(21), and N(31) (Å). [d] Displacement of Mo atom from the equatorial plane defined by O(2), O(3), N(21), and N(31) (Å). [e] Dihedral angle between the plane of the phenolate ring (C1−C6) and the plane defined by Mo(1), N(11), and B(1) (deg).

such as hexane and ethers. Correct microanalyses were obtained for all three compounds. Positive ion ESI-MS results revealed a peak cluster attributable to the cobaltocenium cation (*m*/*z* 189.0) while negative ion ESI-MS revealed a peak cluster for the parent ion, $[M]^-$; these ions are observed even under very low cone voltages, consistent with their presence in the compounds rather than their formation upon electrospray ionization.

The infrared spectra of the complexes exhibited bands assignable to the $\nu_s(MoO_2)$ and $\nu_{as}(MoO_2)$ vibrational modes at about 895 and 790 cm^{-1}; these bands were replaced by those of the Mo(VI) analogues (ca. 935 and 900 cm^{-1}) upon exposure of the IR disk to air. The low energies of the $\nu(MoO_2)$ bands are consistent with the occupation of the delocalized, three-center (MoO_2) π^* orbital by the unpaired electron.[42] Bands characteristic of the Tp^{iPr} (ν(BH) 2439−2498 cm^{-1}, ν(CN) ca. 1508 cm^{-1}) and phenolate (ν(CO) ca. 1570 cm^{-1}, $\nu(CC)_{ring}$ ca. 1260 cm^{-1}) ligands were also present. Again, the substitution patterns of the phenol co-ligands are evident from the fingerprint region (900−680 cm^{-1}).[59] The carbonyl functional groups give rise to characteristic bands at about 1644−1656 cm^{-1}; these values are slightly lower than those found in their dioxo-Mo(VI) precursors. Interestingly, although they occur at the same energy in the Mo(VI) and Mo(V) complexes, the ν(N−H) IR bands are broader and less intense in the latter; this is a strong indication of a higher degree of H-bonding in the Mo(V) complexes.[68]

(68) Silverstein, R. M.; Bassler, C. G.; Morrill, T. C. *Spectrophotometric Identification of Organic Compounds*, 4th ed.; Wiley: New York, 1981.

Table 3. EPR Parameters for **5**−**7** and Related Complexes

R	g_{iso}	A_{iso}[a]	g_1	g_2	g_3	$\langle g \rangle$
Ph (**5**)	1.908	45.2	1.989	1.925	1.810	1.908
4-C_6H_4Cl (**6**)	1.907	45.6	1.988	1.924	1.810	1.907
4-C_6H_4OMe (**7**)	1.907	44.6	1.988	1.925	1.808	1.907
$[Tp^*MoO_2(SPh)]^-$ [b]	1.920	41.4	1.991	1.931	1.843	1.922
$[Tp^{iPr}MoO_2(SPh)]^-$ [b]	1.920	40.6	1.994	1.938	1.842	1.925
$[Tz^*MoO_2(SPh)]^-$ [b]	1.923	40.0	1.994	1.936	1.844	1.925
$[MoO_2(L\text{-}N_2)_2]^-$ [c]	1.942	49.0	1.963	1.945	1.917	1.942

[a] A_{Mo} in units of 10^{-4} cm^{-1}, except for last entry in Gauss. [b] Refs 41 and 42. [c] Ref 46.

Compounds **5**−**7** are EPR-active and give rise to strong signals typical of mononuclear, dioxo-Mo(V) complexes; EPR data are presented in Table 3, and representative spectra are shown in Figure 3. Thus, all complexes display a broad isotropic (solution) spectrum with $g_{iso} \sim 1.908$ at room temperature (see Figure 3a). The dominant central feature is associated with Mo isotopomers with nuclear spins $I_{Mo} = 0$ (natural abundance = 75%). The six satellite peaks, only two of which are clearly evident, are due to hyperfine coupling to $^{95,97}Mo$ nuclei ($I_{Mo} = 5/2$, 25%). The central and low g satellite peaks are not immediately obvious because of overlap with the principal band or because of the effects of g and A strain.[42] The low temperature, frozen-glass EPR spectra for these complexes display rhombic signals where $g_1 \neq g_2 \neq g_3$ and the average g-values correspond closely to the isotropic g-values obtained from the solution spectra (see Figure 3b). Both the isotropic and anisotropic g-values obtained for these complexes differ from those obtained for the series $[CoCp_2][Tp^xMoO_2(SPh)]$,[41,42] and this may

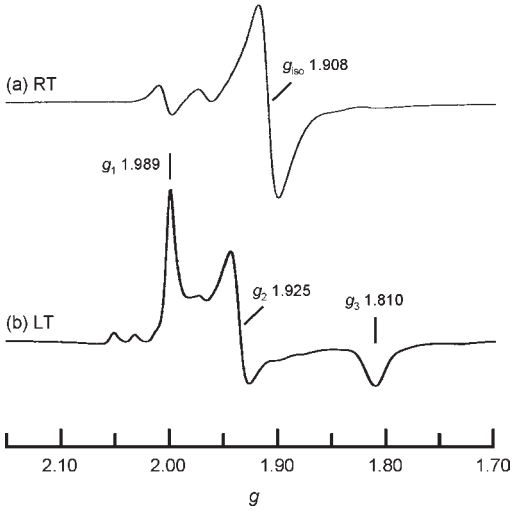

Figure 3. EPR spectra of compound **5** in 10:1 THF/MeCN at (a) room temperature and (b) low temperature (frozen sample in liquid nitrogen).

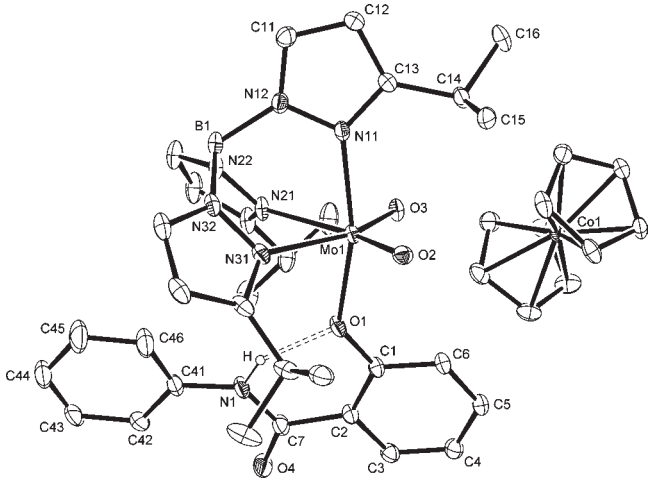

Figure 4. ORTEP projection for an ion-pair of **5** (see Experimental Section for details).

be attributed to the differences in the covalency of the Mo−O and Mo−S bonds.

Electrochemistry. All complexes exhibited three reversible waves assignable to Mo^{VI}/Mo^{V} (see Experimental Section), $[CoCp_2]^+/CoCp_2$ (E = −0.94 V) and $CoCp_2/[CoCp_2]^-$ (E = −1.88 V) couples. The single, reversible, one-electron oxidation of Mo(V) occurred in the potential range −0.598 to −0.565 V versus SCE, values which are similar to those obtained for the reduction of the Mo(VI) counterparts (vide supra).

Crystal Structures. The crystal structures of compounds **5**−**7** were determined by X-ray diffraction. Crystallographic data and selected bond distances and angles are presented in Tables 1 and 2, respectively. The ion-pair in **5** (Figure 4) is representative of all three compounds (ORTEP projections of **6** and **7** are provided in the Supporting Information). The discrete $[CoCp_2]^+$ cations adopt eclipsed conformations with the short Co−C distances typical of the cation (av. Co−C = 2.025−2.035 Å, cf. 2.096(8) Å for $CoCp_2$[69]). The discrete, six-coordinate anions exhibit distorted octahedral coordination geometries and a donor set composed of mutually *cis* oxo and O-donor phenolate ligands, and a tridentate, N_3-donor *fac*-Tp^{iPr} ligand. The general structures of the anions resemble those of their Mo(VI) counterparts, but there are important differences in the metrical parameters.

The Mo=O distances range from 1.724(4)−1.759(4) Å and are significantly longer than those of the Mo(VI) counterparts (1.684(4)−1.7042(13) Å) and the previously reported distances of 1.696−1.705 Å for closely related Mo(VI) complexes.[38,52,61] They are comparable to the Mo=O distances (1.742(9) Å) reported for $[CoCp_2]$-[Tz*MoO_2(SPh)] by Xiao et al.[41,42] The lengthening and equivalence of the Mo=O distances in these Mo(V) complexes are consistent with a principally metal-based, three-centered π^* SOMO. The Mo(1)−O(1) distances range from 2.054(2) to 2.0793(15) Å, with an average of 2.065 Å; these values are longer than those in the Mo(VI) analogues (1.938(3)−1.965(4) Å). The Mo(1)−N(21) and Mo(1)−N(31) distances lie in the ranges 2.369(2)−2.393(4) and 2.312(3)−2.3767(19) Å, respectively, being longer than the Mo(1)−N(11) distances of 2.203(3)−2.207(4) Å because of the trans influence of the oxo ligands. The Mo atom is considerably closer to the O_3-plane (ca. 0.81 Å) than the N_3-plane of the Tp^{iPr} ligand (ca. 1.51 Å) (Table 2). The Mo atom is about 0.046 Å from the mean equatorial plane defined by O(2), O(3), N(21), and N(31), the displacement being toward the phenolate oxygen atom (Table 2).

The O(2)−Mo(1)−O(3) angles, which range from 111.77(17) to 112.75(12)°, are substantially larger than the corresponding values in the Mo(VI) analogues (99.13(9)−101.58(15)°) and related Mo(VI) complexes.[38,52,61] This increase is consistent with a greater repulsion between the d^1 electron and the MoO_2 π-electrons upon reduction. In the solid state, the phenolate ring is proximal to the terminal oxo ligands and the 2-R group is directed toward a cleft in the Tp^{iPr} ligand, being nestled between the two isopropyl groups on the pyrazolyl units trans to the oxo ligands. This structure is exhibited by all complexes **5**−**7** and all these molecules have Mo(1)−O(1)−C(1) angles of about 131−135°. The ipso ring carbon lies beneath the MoO_2 plane, and the 6-C*H* projects toward and lies in close contact with the oxo ligands (O···H−C ca. 2.8 Å). The phenolate ring is displaced considerably from the pseudo-mirror plane in all three complexes.

All the complexes exhibit an intramolecular H-bond involving the amido N(1)−H group and the phenolate oxygen O(1), that closes a six-membered ring incorporating these atoms and C(1), C(2), and C(7). The N(1)···O(1) distances range from 2.584(4)−2.606(6) Å while their H···O(1) distances are about 1.874 Å; here, the N(1)−H···O(1) angles are about 145°. The pseudo six-membered ring (R*) resulting from the H-bonding interaction between N(1)−H···O(1) is almost planar, the root mean squared (*rms*) displacements of the fitted atoms being 0.0239, 0.149, and 0.072 Å for complexes **5**−**7**, respectively. Incidentally, the H atom is the most out-of-plane atom from the planes in all cases. A complete listing of the N(1)−H···O(1) bond lengths and angles are presented in the Supporting Information. Furthermore, the three rings C_6(phenolate), C_6(R), and R* are almost coplanar to each other with **6** having the greatest

(69) Buender, W.; Weiss, E. *J. Organomet. Chem.* **1975**, *92*, 65–68.

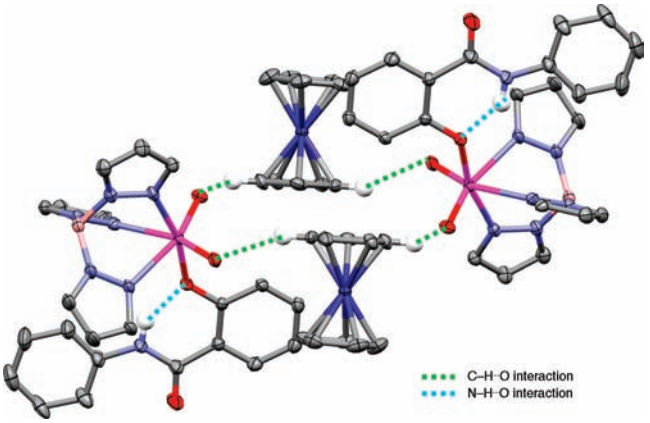

Figure 5. Crystal packing (dimeric) in **5** (and similarly, **7**) resulting from C−H···O interactions (only the H atoms involved in the interactions are shown).

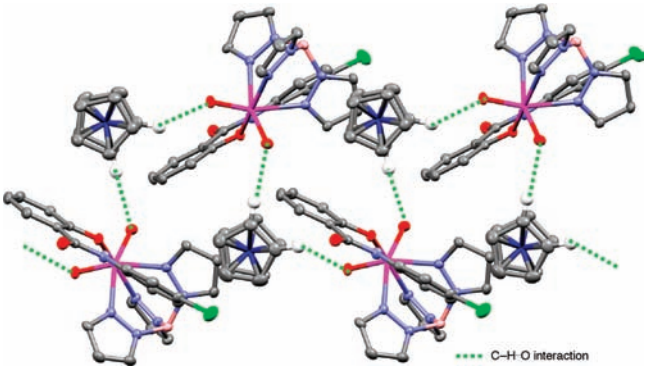

Figure 6. Crystal packing (extended chains) in **6** resulting from C−H···O interactions (only the H atoms involved in the interactions are shown).

dihedral angle between the C_6(R) and R* planes. The extent of coplanarity may have a subtle impact on the electronic delocalization and stabilization of the compounds.

In addition to the N(1)−H···O(1) intramolecular H-bonds that are observed in the crystal structures of **5**−**7**, there are also intermolecular C_{Cp}−H···O_{Mo} H-bond interactions present within the crystal lattice. The C_{Cp}···O_{Mo} distances range from 3.043(5)−3.434(3) Å while the H_{Cp}···O_{Mo} distances range from about 2.266(3)−2.520(2) Å; both values are typical of H-bond distances.[63,64] The C_{Cp}−H···O_{Mo} angles for these complexes range from 129.90(36)−172.12(16)°, the greatest deviation from linearity being observed in the packing of complex **6**. In the case of **5** and **7**, each Mo=O group is H-bonded to a C−H moiety on the Cp ring of the cobaltocenium cation; each $[CoCp_2]^+$ bridges two molybdenum units, generating a dimeric structure with a center of inversion as illustrated in Figure 5. On the other hand, the crystal packing in **6** is distinct from that of **5** and **7**, with each $[CoCp_2]^+$ bridging two separate molybdenum units, creating an extended polymeric chain structure (Figure 6). The formation of this extended structure is supported by an elongation of the C−H···O bonds (ca. 3.37 vs 3.12 Å) and a wider C_{Cp}−H···O(3) bond angle of about 170°. A complete listing of the C_{Cp}−H···O_{Mo} bond lengths and angles are presented in the Supporting Information.

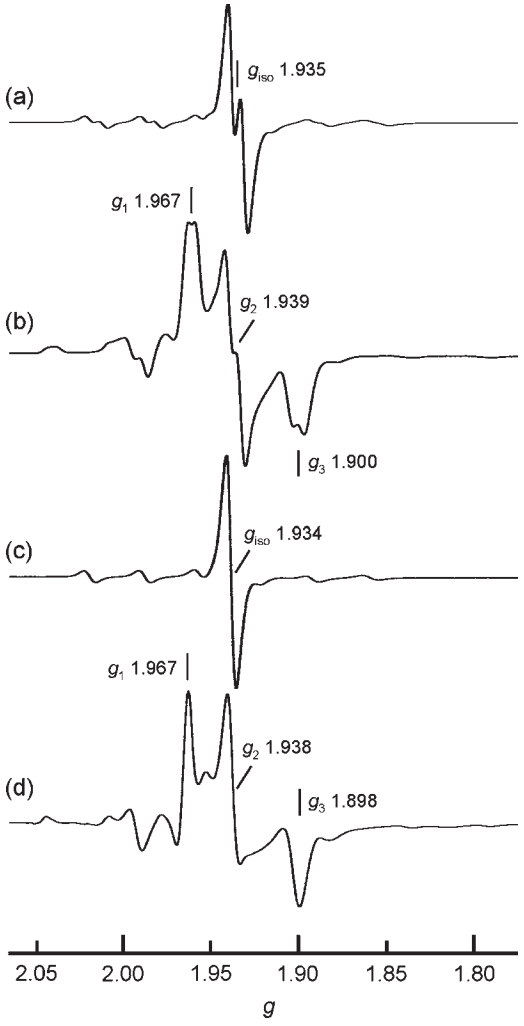

Figure 7. EPR spectra of **8** at room temperature (a) and in frozen glass (b); EPR spectra of $Tp^{iPr}MoO(OD)(2\text{-}OC_6H_4CONHPh)$ (**8**-OD) at room temperature (c) and in frozen glass (d). Solvent: 1:1 THF/toluene.

Protonation of Dioxo-Mo(V) Complexes. The incorporation of the salicylanilide ligands into the title complexes was aimed at stabilizing $[Mo^VO(OH)]^{2+}$ complexes through H-bonding, permitting their quantitative formation and facilitating their existence in frozen glass media. This approach appears to have been successful, albeit with judicious choice of acid.

The use of "strong" acids, for example, triflic acid, tetrafluoroboric acid, and *p*-toluenesulfonic acid, to protonate the dioxo-Mo(V) anions resulted in decomposition to dark blue or green materials that are highly soluble in water but largely insoluble in organic solvent; these are presumed to be reduced polyoxomolybdate complexes produced by the presence of adventicious water. Lutidinium tetrafluoroborate, [lutH]BF_4, was eventually identified as a suitable water-free, proton donor for the *cis*-dioxo-Mo(V) complexes. Reactions were carried out in 1:1 THF/toluene to facilitate the clean generation of solutions of $Tp^{iPr}MoO(OH)(2\text{-}OC_6H_4CONHR)$ (R = Ph (**8**), 4-C_6H_4Cl (**9**), 4-C_6H_4OMe (**10**)) following removal of the precipitated $[CoCp_2]BF_4$ (eq 4).

$$[CoCp_2][Tp^{iPr}MoO_2(2\text{-}OC_6H_4CONHR)] + [lutH]BF_4 \rightarrow \mathbf{8}\text{−}\mathbf{10} + [CoCp_2]BF_4 + lut \quad (4)$$

Table 4. EPR Data for **8**−**10**, Their Deuterated Counterparts (-OD) and Low pH, Mo(V) Forms of Sulfite Oxidase (SO)

R	g_{iso}	A_{iso}[a]	g_1	g_2	g_3	$\langle g \rangle$
Ph (**8**)	1.935	48.13 11.54	1.967	1.939	1.900	1.935
8-OD	1.934	47.88	1.967	1.938	1.898	1.934
4-C_6H_4Cl (**9**)	1.934	48.09 11.55	1.968	1.937	1.900	1.935
9-OD	1.934	47.73	1.967	1.939	1.898	1.934
4-C_6H_4OMe (**10**)	1.934	48.06 11.36	1.968	1.936	1.899	1.934
10-OD	1.934	47.87	1.968	1.940	1.899	1.935
chicken SO[b]			2.0037	1.9720	1.9658	1.9805
human SO[b]			2.0037	1.9720	1.9658	1.9805
A. thaliana SO[b]			2.006	1.975	1.968	1.983

[a] A_{Mo} (∼48) and A_H (∼ 11) in units of 10^{-4} cm^{-1}. [b] Ref 36 and references therein.

The reactions were followed by EPR spectroscopy. In experiments involving the R = Ph derivative, for example, the initial broad signal from **5** (g_{iso} = 1.908) was rapidly replaced by a well-defined proton-coupled doublet (g_{iso} = 1.935; $A_{iso}(^{95,97}Mo) = 48.13 \times 10^{-4}$ cm^{-1}; $A_{iso}(^1H) = 11.54 \times 10^{-4}$ cm^{-1}) (Figure 7a). The anisotropic spectra revealed rhombic signals where $g_1 \neq g_2 \neq g_3$ (Figure 7b). The averaged anisotropic *g*-values correspond closely to the isotropic *g*-values obtained from the solution spectra. In addition, the expected superhyperfine coupling of the electron to the proton was still evident on all three features, consistent with the persistence of the $[Mo^VO(OH)]^{2+}$ species at low temperature in frozen glasses; this observation is unprecedented and sets the stage for a more detailed examination of proton coupling to Mo(V). Deuterium exchange using D_2O resulted in the collapse of the doublet and the formation of an apparent singlet with six Mo hyperfine lines (g_{iso} = 1.934; $A_{iso}(^{95,97}Mo) = 47.88 \times 10^{-4}$ cm^{-1}) (Figure 7c). The anisotropic spectrum is again rhombic, but the coupling to ^1H is missing because of deuterium exchange (Figure 7d). It was also observed that the proton coupling was better resolved in less polar solvents, that is, a 1:1 THF/toluene mixture, than say 10:1 THF/MeCN or CH_2Cl_2. The EPR parameters established for the *cis*-(hydroxo)oxo-Mo(V) complexes are provided in Table 4.

The anisotropic *g*-values of complexes **8**−**10** are rather insensitive to co-ligand substituents and are markedly different from those obtained for the various SO enzymes (Table 4). The differences in the *g* values of the model complexes and the enzymes are likely to be due to the differences in metal−ligand covalency, the softer S-donor ligands at the enzyme active site being more covalent that the hard N- and O-donors of these model complexes. In spite of this, the magnitude of isotropic superhyperfine coupling to ^1H (ca. 11×10^{-4} cm^{-1}) is within the range reported for the enzymes.[36] It is not known whether the $NH\cdots O_{phenolate}$ H-bond persists in these complexes or whether the NH group interacts with and stabilizes the hydroxo ligand. It is hoped that more detailed spectroscopic studies of these complexes will provide insights into these aspects of their structures.

Summary

This paper describes the synthesis, characterization, and structural analysis of the *cis*-dioxo-Mo(VI/V) compounds $Tp^{iPr}Mo^{VI}O_2(2\text{-}OC_6H_4CONHR)$ (**1**−**4**) and $[CoCp_2][Tp^{iPr}Mo^VO_2(2\text{-}OC_6H_4CONHR)]$ (**5**−**7**). The rare *cis*-dioxo-Mo(V) complexes are electronically and/or structurally stabilized by an intramolecular H-bond. They were found to be more stable than previously reported complexes of this type and can be handled in air without rapid decomposition. In addition, these complexes can be converted to $Tp^{iPr}MoO(OH)(2\text{-}OC_6H_4CONHR)$ (**8**−**10**) by protonation with lutidinium tetrafluoroborate; significantly, these are the first such species to persist in low temperature frozen glasses. These *cis*-(hydroxo)oxo-Mo(V) compounds are structural and spectroscopic models of the low pH, Mo(V) forms of SO.[36]

Acknowledgment. We thank Mr. Damien C. Clarke for experimental assistance and gratefully acknowledge the financial support from the Australian Research Council, the Donors of the Petroleum Research Fund (administered by the American Chemical Society), and the Albert Shimmins Memorial Fund (for a Writing-up Award).

Supporting Information Available: Crystallographic data in CIF format, ORTEP projections for compounds **2**, **3**, **6**, and **7**, and tables of selected distances and angles for $N(1)-H\cdots O(1)$ and $C_{Cp}-H\cdots O_{Mo}$ H-bonds. This material is available free of charge via the Internet at http://pubs.acs.org.